S. Roy,†
H.-G. Lombart,‡
W. D. Lubell
R. E. W. Hancock
S. W. Farmer

Exploring relationships between mimic configuration, peptide conformation and biological activity in indolizidin-2-one amino acid analogs of gramicidin S*

Author's affiliations:
S. Roy,† H.-G. Lombart‡ and W. D. Lubell
Département de chimie, Université de Montréal, Montréal, Canada; present addresses †MethylGene Inc., Montréal, Canada, ‡Wyeth Research, Cambridge, USA.

R. E. W. Hancock and S. W. Farmer
Department of Microbiology and Immunology, University of British Columbia, Vancouver, Columbia, Canada.

Correspondence to:
Professor *William D. Lubell*
Département de chimie
Université de Montréal
CP 6128, Succursale Cebtre-Ville
Montréal
Québec
Canada H3C 3J7
Tel.: 1-514-343-7339
Fax: 1-514-343-7586
E-mail: lubell@chimie.umontreal.ca

Dates:
Received 25 April 2002
Revised 22 May 2002
Accepted 9 June 2002

To cite this article:
Roy, S., Lombart, H.-G., Hancock, R.E.W., Farmer, S. W. & Lubell, W. D. Exploring relationships between mimic configuration, peptide conformation and biological activity in indolizidin-2-one amino acid analogs of gramicidin S.

*Dedicated to the memory of Professor Henry Rapoport, an outstanding scientist, scholar and mentor.

J. Peptide Res., 2002, **60**, 198–214.

ISSN 1397–002X

Key words: antibiotic peptides; antimicrobial peptide; β-turn; circular dichroism spectroscopy; gramicidin S; indolizidin-2-one amino acid; solid-phase synthesis

Abstract: Indolizidin-2-one amino acids (I^2aas, 6*S*- and 6*R*-**1**) possessing 6*S*- and 6*R*-ring-fusion stereochemistry were introduced into the antimicrobial peptide gramicidin S (GS) to explore the relationships between configuration, peptide conformation and biological activity. Solution-phase and solid-phase techniques were used to synthesize three analogs with I^2aa residues in place of the D-Phe-Pro residues at the turn regions of GS: [(6*S*)-$I^2aa^{4-5,4'-5'}$]GS (**2**), [$Lys^{2,2'}$,(6*S*)-$I^2aa^{4-5,4'-5'}$]GS (**3**) and [(6*R*)-$I^2aa^{4-5,4'-5'}$]GS (**4**). Although conformational analysis of [$I^2aa^{4-5,4'-5'}$]GS analogs **2**–**4** indicated that both ring-fusion stereoisomers of I^2aa gave peptides with CD and NMR spectral data characteristic of GS, the (6*S*)-I^2aa analogs **2** and **3** exhibited more intense CD curve shapes, as well as greater numbers of nonsequential NOE between opposing Val and Leu residues, relative to the (6*R*)-I^2aa analog **4**, suggesting a greater propensity for the (6*S*)-diastereomer to adopt the β-turn/antiparallel β-pleated sheet conformation. In measurements of antibacterial and antifungal activity, the (6*S*)-I^2aa analog **2** exhibited significantly better potency than the (6*R*)-I^2aa diastereomer **4**. Relative to GS, [(6*S*)-$I^2aa^{4-5,4'-5'}$]GS (**2**) exhibited usually 1/2 to 1/4 antimicrobial activity as well as 1/4 hemolytic activity. In certain cases, antimicrobial and hemolytic activities of GS were shown to be dissociated through modification at the peptide turn regions with the (6*S*)-I^2aa diastereomer. The synthesis and evaluation of GS analogs **2**–**4** has furnished new insight into the importance of ring-fusion stereochemistry for turn mimicry by indolizidin-2-one amino acids as well as novel antimicrobial peptides.

As microbial organisms exhibiting clinically significant drug resistance have emerged (1–4) an urgent need has been created for new agents that combat infectious disease by novel modes of action (5–8). Among leads for the development of antibacterial agents, antimicrobial peptides are particularly attractive candidates because they function generally by mechanisms of action that are different from their nonpeptide counterparts (8, 9). Furthermore, antimicrobial peptides offer an economical means for confronting bacterial pathogens, because they can be assembled efficiently from inexpensive amino acid starting materials. For similar reasons, antimicrobial peptide libraries may be synthesized for drug discovery using combinatorial methods of diversification (10). Although the employment of antimicrobial peptides in clinic has been limited because of their nonspecific cytotoxic activities, specifically hemolytic activity (8, 9, 11) analogs that retain high antimicrobial activity, but lose their eukaryotic cell killing activity may be synthesized by altering the natural peptide structure (8, 12). For example, the synthesis of a retroenantio derivative of melittin, the principal toxic component of bee venom, has produced a fully active antibacterial agent that exhibited no hemolytic effects (8). In addition, structural modifications may also be made to improve the metabolic stability and bioavailability of antimicrobial peptides.

Gramicidin S [*cyclo*(Val-Orn-Leu-D-Phe-Pro)$_2$] is a naturally occurring peptide that displays potent antibacterial effects against both gram-negative and gram-positive bacteria (13). Although GS is a topical antibiotic (14, 15), its employment is restricted because of high hemolytic activity, as illustrated by the lysis of red blood cells (11, 13). The antibacterial and hemolytic activities can be dissociated in GS analogs, as demonstrated by the synthesis and analysis of GS derivatives possessing varying ring sizes (11). The antibacterial activity of GS has been shown to be contingent on the peptide conformation in which the D-Phe-Pro residues adopt the central positions of type II′ β-turns that stabilize an antiparallel β-pleated sheet (16). The structure of GS is amphiphatic possessing charged ammonium groups of the ornithine residues projecting from one side of the sheet and neutral hydrophobic residues extending from the opposite side. Although the mode of GS action is not entirely understood, these structural features are believed to enable the peptide to bind to the cell membrane of sensitive microorganisms and thereby cause changes in membrane permeability (16–25).

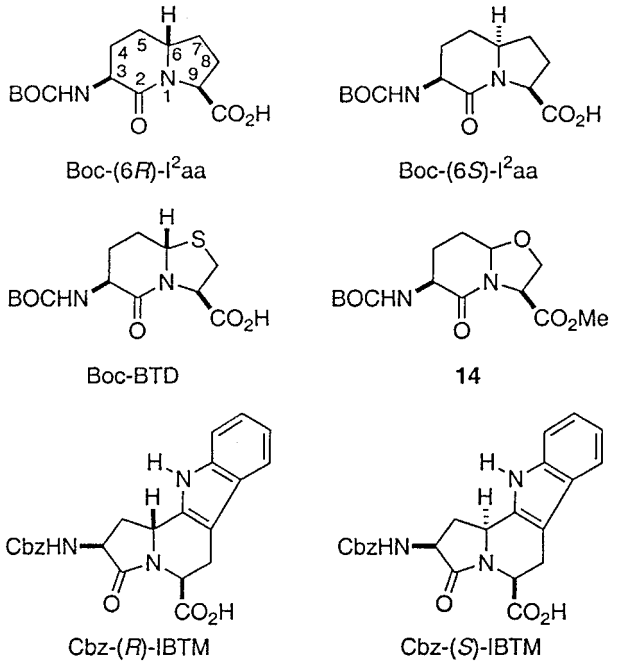

Figure 1. Related indolizidinone amino acids.

Numerous analogs of GS have been synthesized previously with the aim of producing more potent antibiotic peptides (22, 23). Although many structural modifications have resulted in decreased activity, an important exception was found when the thiaindolizidinone amino acid BTD (Fig. 1) (26) was introduced at the turn regions of GS (27, 28). The resulting analogs [BTD$^{4-5,4'-5'}$]GS and [BTD$^{4-5}$]GS possessed spectral characteristics and antibacterial activities similar to that of the native peptide (23, 24). Several rigid dipeptide derivatives have since been used to replace the D-Phe-Pro residues in GS (29–34). Similar antibiotic activity as well as matching spectral properties to that of GS have been suggested as a measurement of the capacity of these rigid dipeptide mimics to serve as surrogates of the $i + 1$ and $i + 2$ residues of type II′ β-turns (29–32).

To study further the influence of structural modification on the activity and specificity of GS, we have employed (6*S*)- and (6*R*)-indolizidin-2-one amino acids (I²aas,(6*S*)- and (6*R*)-**1**; Fig. 1) to prepare three new analogs: [(6*S*)-I²aa$^{4-5,4'-5'}$]GS (**2**) (35) [Lys$^{2,2'}$,(6*S*)-I²aa$^{4-5,4'-5'}$]GS (**3**) and [(6*R*)-I²aa$^{4-5,4'-5'}$]GS (**4**). With an expedient method for synthesizing enantiopure I²aas in hand (36, 37) we selected to synthesize GS analogs using both the (3*S*, 6*S*, 9*S*)- and (3*S*, 6*R*, 9*S*)-diastereomers to examine the consequence of ring-fusion stereochemistry on β-turn geometry and peptide conformation. Increased metabolic stability was expected

to be an added benefit of studying the all carbon indolizidinone analogs which do not possess the masked aldehyde found in their thiaindolizidinone counterparts. By testing [$I^2aa^{4-5,4'-5'}$]GS analogs **2**–**4** for activity against yeast, gram-positive and gram-negative bacteria, as well as for hemolytic activity, we have investigated further the relationship between peptide conformation and antimicrobial activity and specificity.

Results

Synthesis

A convergent approach and solution-phase techniques were used to synthesize [(6*S*)-$I^2aa^{4-5,4'-5'}$]GS (**2**, Fig. 2) (35). The starting material, enantiopure (3*S*, 6*S*, 9*S*)-indolizidinone *N*-(Boc)amino acid (6*S*)-**1** was efficiently synthesized via our

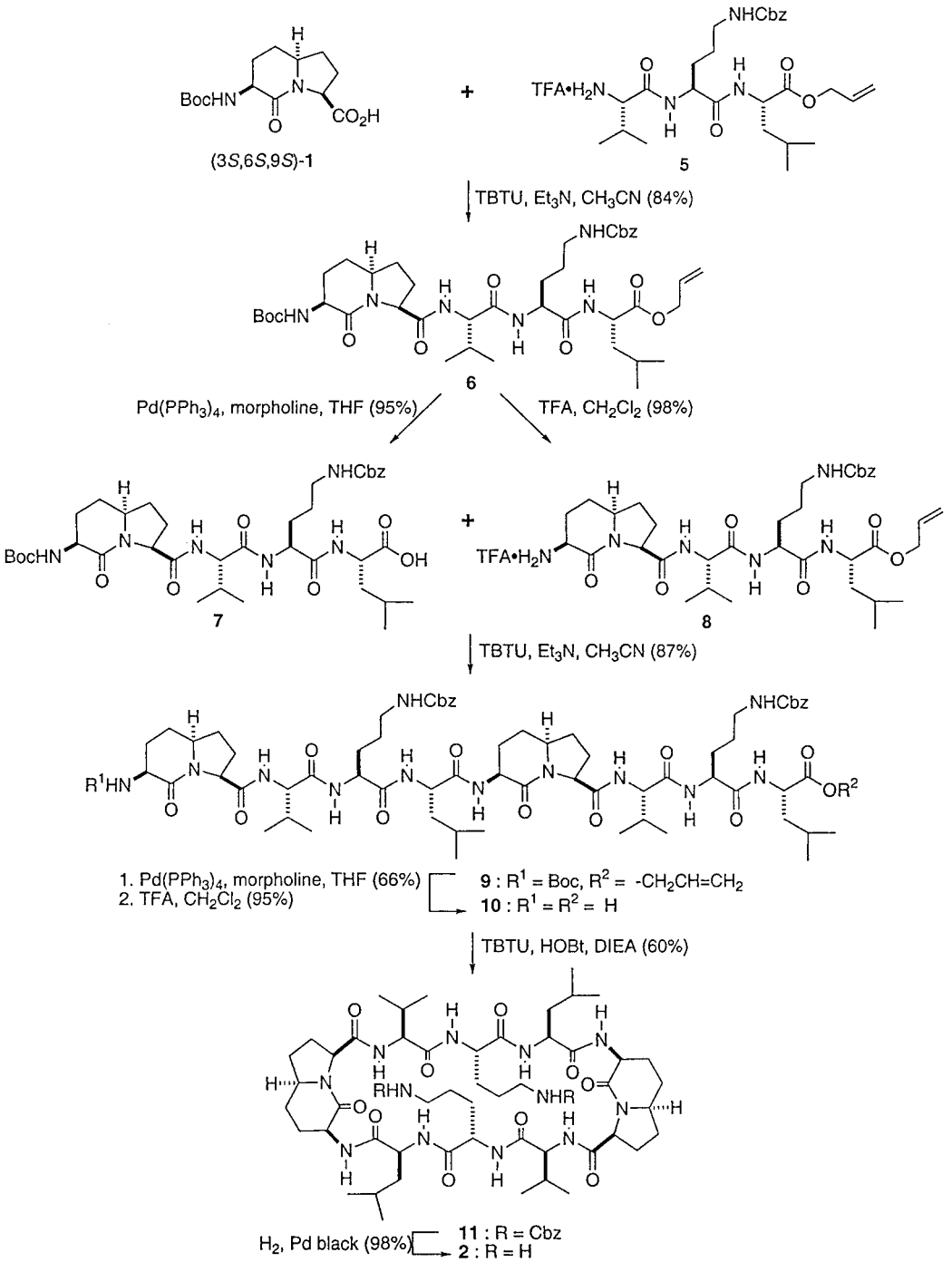

Figure 2. Synthesis of peptide **2**.

Claisen condensation/reductive amination/lactam formation sequence from glutamic acid as chiral educt (36, 37). The tripeptide **5**, Val-(Cbz)Orn-Leu-O-allylTFA, was synthesized from L-leucine allyl ester *p*-toluenesulfonate (38), L-N^{α}-(Boc)-N^{δ}-(Cbz)ornithine and L-*N*-(Boc)valine in four steps and 65% overall yield using benzotriazol-1-yl-1,1,3,3-tetramethyluronium tetrafluoroborate (TBTU) for peptide couplings (39–41), TFA for Boc group removals, and chromatography on silica gel to isolate several intermediates as described in detail in the experimental section.

Indolizidinone amino acid **1** was coupled to tripeptide **5** using TBTU and Et_3N in CH_3CN to provide tetrapeptide **6**, Boc-I²aa-Val-(Cbz)Orn-Leu-O-allyl, in 84% yield after chromatography on silica gel with EtOAc in hexane as eluant. The pentapeptide material was then divided into two portions. In one pot, the C-terminal allyl ester of **6** was deprotected with $Pd(PPh_3)_4$ and morpholine in THF to furnish carboxylic acid **7** in 95% yield (42). In another pot, the N-terminal Boc group of **6** was removed quantitatively with TFA in CH_2Cl_2 to give amine **8** as its trifluoroacetate salt. The two pentapeptides, **7** and **8**, were then coupled with TBTU to furnish the protected decapeptide **9**, Boc-I²aa-Val-(Cbz)Orn-Leu-I²aa-Val-(Cbz)Orn-Leu-O-allyl, in 87% yield. Similar deprotection conditions were then used to remove the allyl ester and Boc groups of peptide **9** in 66 and 95% respective yields and furnished linear precursor **10**. Macrocyclization was performed at high dilution using TBTU and 1-hydroxybenzotriazole (HOBt) with diisopropylethylamine in DMF and was monitored by analytical HPLC which showed complete reaction after 1 h. A crude product was isolated in 85% recovery after aqueous work-up. Subsequent purification using reverse-phase HPLC and lyophilization of the collected fractions gave the pure protected GS analog **11** in 60% yield ($m/z = [MH]^+$ 1282.3). No traces of dimeric nor polymeric products were observed by MS analysis of the crude cyclization material. Hydrogenolysis of the Cbz protecting groups, using Pd-black as catalyst in MeOH·HCl (27), gave quantitatively [(6*S*)-I²aa$^{4-5,4'-5'}$]GS (**2**, $m/z = [M]^+$ 1013.7) as a white hydrochloride salt after isolation by reverse phase HPLC (Fig. 2).

Solid-phase strategies were used to prepare [Lys$^{2,2'}$,(6*S*)-I²aa$^{4-5,4'-5'}$]GS **3** and [(6*R*)-I²aa$^{4-5,4'-5'}$]GS **4** on oxime resin to develop an approach more amenable for library production (Fig. 3). The linear peptides were synthesized on the solid support and removed by intramolecular cyclization cleavage (43–46). In consideration of the biosynthetic pathway for the synthesis of GS (23), Boc-Leu-OH was first coupled onto oxime resin using DCC and ethyl-2-(hydroxyimino)-2-cyanoacetate (EACNOx) as an additive to minimize racemization (47). The Boc groups were removed with TFA and peptide couplings were effected using N-(Boc)amino acids (Cbz protection for Orn and Lys side chains), TBTU and diisopropylethylamine (DIEA). After elongation of the linear peptide on solid support, the N-terminal amine was deprotected using TFA and neutralized with DIEA. Cyclization and cleavage of *cyclo*(Val-Lys(Z)-Leu-(6*S*)-I²aa)$_2$ **12** and *cyclo*(Val-Orn(Z)-Leu-(6*R*)-I²aa)$_2$ **13** were accomplished by treating resins containing the linear peptide with DIEA and AcOH in, respectively, DMF and CH_2Cl_2. The crude protected peptides were then purified by ion-exchange chromatography and reverse-phase HPLC, respectively, to afford **12** ($m/z = [MH]^+$ 1310.2) and **13** ($m/z = [MH]^+$ 1281.8), albeit in 10 and 2% respective yields based on initial loading of the resin. The Cbz groups were then removed by hydrogenolysis using Pd-black as catalyst in MeOH·HCl to provide [Lys$^{2,2'}$,(6*S*)-I²aa$^{4-5,4'-5'}$]GS (**3**, $m/z = [MH]^+$ 1041.4) and [(6*R*)-I²aa$^{4-5,4'-5'}$]GS (**4**, $m/z = [MH]^+$ 1013.7), both in 98% yield as white hydrochloride salts after isolation by reverse-phase HPLC.

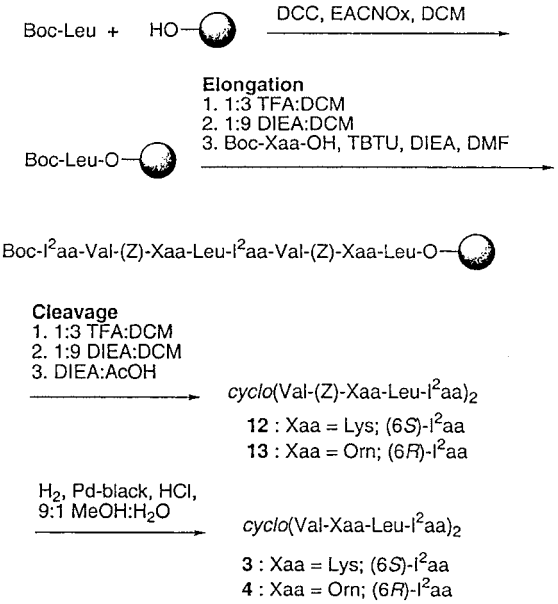

Figure 3. Synthesis of [I²aa$^{4-5,4'-5'}$]GS analogs 3 and 4.

Circular dichroism spectral analysis

The circular dichroism (CD) spectra for GS and peptides **2–4** were measured in methanol and water (Fig. 4; 48, 49). In methanol, the spectral characteristics of analogs **2–4** were similar to those of GS indicating that they adopted similar conformations. All exhibited a negative maximum situated at ≈207 nm, a positive maximum at ≈195 nm and a negative shoulder at ≈225 nm in methanol. Similar spectra

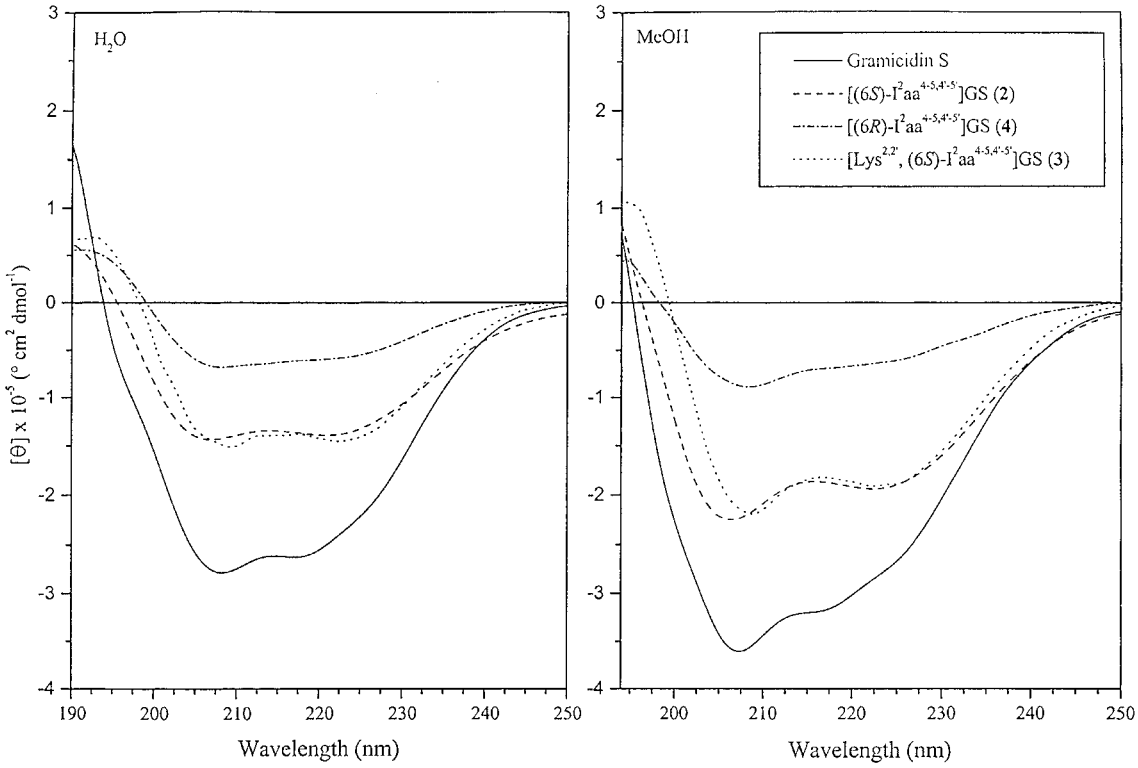

Figure 4. Circular dichroism spectra for [$I^2aa^{4-5,4'-5'}$]GS analogs 2–4.

were measured in water; however, nearly equal negative band intensities were observed for the maximum and the shoulder in the [$I^2aa^{4-5,4'-5'}$]GS analogs **2–4**. Relative to the band intensities exhibited by peptides **2–4**, GS exhibited a significantly lower negative maximum, which has been suggested to result from the presence of the aromatic Phe chromophores that were removed in the I^2aa analogs (27). Furthermore, (6*S*)-I^2aa analogs **2** and **3** exhibited stronger negative maximum relative to (6*R*)-I^2aa analog **4**, which may be indicative of the better propensity of the concave (6*S*)-I^2aa diastereomer for stabilizing the antiparallel β-pleated sheet conformation characteristic of GS.

NMR spectral analysis

The conformations of [$I^2aa^{4-5,4'-5'}$]GS analogs **2–4** were further investigated using NMR spectroscopy. Assignment of the proton signals was made using 2D NMR experiments and was simplified because of C_2 symmetry (50). For example, a combination of TOCSY and COSY spectra was employed to identify the NH and Cα, as well as the side-chain protons of the Val, Leu, Orn and Lys residues. Moreover, the protons at positions 3, 4 and 5 of the I^2aa residue could be identified by the combination of TOCSY and COSY spectra. However, assignments for the protons at positions 6, 7, 8 and 9 of the I^2aa residue were made using HMQC and NOESY spectra.

Sequential through-space couplings for antiparallel β-pleated sheet conformations are characterized by strong NOEs between the NH and Cα protons of adjacent residues combined with weak NOEs between the NH protons of adjacent residues (50). By integration of the cross-peaks of spectra obtained from NOESY experiments with **2–4**, we could establish that all three analogs possessed such characteristic through-space couplings (Table 1). In the cases of [(6*S*)-$I^2aa^{4-5,4'-5'}$]GS (**2**) and [(6*R*)-$I^2aa^{4-5,4'-5'}$]GS (**4**), the Val, Orn and Leu residues, all exhibited strong NOEs between the NH and Cα protons and weak NOEs between the NH protons of their respective adjacent residues. Similarly, the NOESY spectra for [$Lys^{2,2'}$,(6*S*)-$I^2aa^{4-5,4'-5'}$]GS (**3**) exhibited strong NOEs between the NH and Cα protons of the adjacent Val, Lys and Leu residues; however, weak to medium intensity NOEs were observed between the NH protons of the adjacent residues. In general, all three analogs exhibited sequential NOEs that were consistent with an antiparallel β-pleated sheet conformation.

The antiparallel β-pleated sheet conformation positions residues on opposite sides of the sheet in close enough proximity to exhibit nonsequential through-space coupling. The extent of such nonsequential through-space couplings may be indicative of the stability of the antiparallel

Table 1. **Sequential NOEs between backbone NH and Cα protons in I^2aa-GS analogs 2–4 in water**

Proton(s)	NOE intensity [(6*S*)-I^2aa]GS **2**	[Lys, (6*S*)-I^2aa]GS **3**	[(6*R*)-I^2aa]GS **4**
Val-Cα Orn(Lys)-NH	strong	strong	strong
Val-NH Orn(Lys)-NH	weak	weak	weak
Orn(Lys)-Cα Leu-NH	strong	strong	strong
Orn(Lys)-NH Leu-NH	weak	medium	weak
Leu-Cα I^2aa-NH	strong	strong	strong
Leu-NH I^2aa-NH	weak	medium	weak

Table 2. **Non-sequential NOEs between opposing Val and Leu residues in I^2aa-GS analogs 2–4**

Proton(s) Valine	Leucine	NOE intensity [(6*S*)-I^2aa]GS **2**	[Lys, (6*S*)-I^2aa]GS **3**	[(6*R*)-I^2aa]GS **4**
NH	NH	weak	weak	weak
NH	Cα	weak	–	–
NH	Cβ	–	medium	–
NH	Cβγ[a]	weak	–	–
NH	Cγ	–	weak	–
Cα	NH	weak	medium	–
Cβ	NH	medium	medium	weak
Cγ	NH	weak		–
Cγ	Cβγ[a]	medium		–

a. Overlapping signals.

β-pleated sheet conformation. In the case of [$I^2aa^{4-5,4'-5'}$]GS analogs **2–4** (Table 2), the number and the intensity of the NOEs between opposing residues varied significantly with the stereochemistry of the I^2aa residue and the chain-length of the basic amino acid residue (Orn vs. Lys, Table 2). For example, two medium- and five weak-intensity NOEs were observed between the opposing Val and Leu residues in [(6*S*)-$I^2aa^{4-5,4'-5'}$]GS (**2**). Three medium- and two weak-intensity NOEs were observed between the opposing Val and Leu residues in [$Lys^{2,2'}$,(6*S*)-$I^2aa^{4-5,4'-5'}$]GS (**3**). In contrast, only two weak intensity NOEs were observed between the opposing Val and Leu residues in [(6*R*)-$I^2aa^{4-5,4'-5'}$]GS (**4**). Based on the number and intensity of the through-space couplings between opposing residues, the peptide possessing the concave (6*S*)-I^2aa diastereomer appeared to adopt more favorably an ideal antiparallel β-pleated sheet conformation relative to its convex (6*R*)-I^2aa counterpart.

The temperature coefficients for the amide protons in peptides **2–4** were measured to provide additional evidence for an antiparallel β-pleated sheet conformation (51). Values > -3 p.p.b./K have been suggested to indicate a solvent shielded amide proton engaged in an intramolecular hydrogen bond in DMSO (51). In this respect, the amide protons for the Val and Leu residues in GS exhibited respective temperature coefficient values of −1.6 p.p.b./K and −2.8 p.p.b./K indicative of hydrogen bonded and solvent shielded amide protons (28). However, the amide proton of the Orn residues exhibited a temperature coefficient values of −5 p.p.b./K indicative of solvent exposed protons (28). Similar trends were observed for the temperature coefficients of the amide protons in the [$I^2aa^{4-5,4'-5'}$]GS analogs **2–4** that suggested an antiparallel β-pleated sheet conformation (Table 3).

Finally, the values of the coupling constants between the amino acid α- and amide protons ($^3J_{NH\text{-}C\alpha H}$) were measured to provide additional information on the local conformation of each residue in the [$I^2aa^{4-5,4'-5'}$]GS analogs **2–4** (Table 4). The $^3J_{NH\text{-}C\alpha H}$ values should be > 7.0 Hz for residues in an extended antiparallel β-pleated sheet conformation (50, 52). Such values were exhibited by the Val, Orn and Leu residues in GS (28), and [$I^2aa^{4-5,4'-5'}$]GS analogs **2** and **4**. In the case of [$Lys^{2,2'}$,(6*S*)-$I^2aa^{4-5,4'-5'}$]GS **3**, the values of the Val and Leu residues were measured, respectively, at 8.3 and 6.9 Hz; however, the Lys residue exhibited a $^3J_{NH\text{-}C\alpha H}$ value of 5.3 Hz. The lower value exhibited by the Lys residue

Table 3. **Amide temperature coefficient values ($\Delta\delta/\Delta T$, ppm 10^3/K) in DMSO (water) for GS and I^2aa-GS analogs 2–4**

Residue	GS[a]	[(6*S*)-I^2aa]GS **2**	[Lys, (6*S*)-I^2aa]GS **3**	[(6*R*)-I^2aa]GS **4**
Val	−1.6	−2.6	(−3.7)	−1.3 (0.05)
Orn (Lys)	−5	−7.5	(−5.9)	−5.5 (−8.3)
Leu	−2.8	−3.9	(−2.7)	−3.3 (−4.2)
D-Phe (I^2aa)	−7.4	−8.8	(−11.2)	−6.5 (−9.4)

a. Values taken from Ref. 28.

Table 4. **Coupling constant ($^3J_{NH\text{-}C\alpha H}$) values (Hz) for GS in DMSO and I^2aa-GS analogs 2-4 in water**

Residue	GS[a]	[(6*S*)-I^2aa]GS **2**	[Lys, (6*S*)-I^2aa]GS **3**	[(6*R*)-I^2aa]GS **4**
Val	9.7	8.5	8.3	9.3
Orn (Lys)	8.9	8.6	5.3	9.3
Leu	8.6	8.6	6.9	9.3
D-Phe (I^2aa)	7.3	7.3	7.2	6.9

a. Values taken from Ref. 28.

suggests that the lengthening of the side-chain of the basic residue perturbs the ideal antiparallel β-pleated sheet geometry, which may be due to intramolecular hydrogen bonding between the charged Lys ω-ammonium group and a carbonyl of the peptide backbone. The spin-spin coupling constant for the $i + 1$ and $i + 2$ residues of a turn structure have similarly been used to assign peptide backbone geometry (52). The $^3J_{NH\text{-}C\alpha H}$ value around 7 Hz has been reported for the $i + 1$ residue in a type II′ β-turn (52), as observed for the D-Phe residue in GS (28), as well as for the I^2aa residues in analogs **2–4**.

In sum, the NOEs, amide temperature coefficients and spin-spin coupling constant values ($^3J_{NH\text{-}C\alpha H}$) for analogs **2–4**, all were consistent with the β-turn/antiparallel β-pleated sheet conformation adopted by GS. Subtle differences in the spectroscopic data for analogs **2–4** were observed that may indicate their relative efficiency in adopting ideal antiparallel β pleated sheet conformations. For example, the number and intensity of the nonsequential NOE between the opposing Val and Leu residues diminished significantly as the ring-fusion stereochemistry was changed from 6*S* to 6*R* in analogs **2** and **4**, which may indicate that the concave (6*S*)-indolizidin-2-one diastereomer is better suited for stabilizing the sheet conformation relative to its convex (6*R*)-counterpart. Similarly, the number of the nonsequential NOE between the opposing Val and Leu residues was reduced as the Orn in analog **2** was changed to Lys in **3**. This reduction in NOE between opposing residues combined with the lower $^3J_{NH\text{-}C\alpha H}$ value exhibited by the Lys residue in **3**, both indicate that the Orn residue may be more ideally suited in the antiparallel β-pleated sheet geometry relative to its homolog Lys.

Anti-microbial and hemolytic activities

The antimicrobial and hemolytic activities of GS and [$I^2aa^{4-5,4'-5'}$]GS analogs **2–4** were compared using liquid-based assays, because in the liquid broth solution-based assay, GS had been found to show activity against gram-negative bacteria as well as antifungal activity, two characteristics that were previously not detected in examinations of GS using the more common agar-based assays (13). The antibacterial and antifungal activities of GS and [$I^2aa^{4-5,4'-5'}$]GS analogs **2–4** are presented as the lowest concentration of compound necessary for > 50% inhibition of the growth of the microorganism (MICs in μg/mL) in Table 5. In general, [$I^2aa^{4-5,4'-5'}$]GS analogs **2–4** exhibited reduced antibacterial and antifungal activities relative to those exhibited by GS. Antimicrobial activity of [$I^2aa^{4-5,4'-5'}$]GS analogs **2–4** was contingent on ring fusion stereochemistry and the concave 6*S*-I^2aa diastereomers **2** and **3** exhibited greater activity that the 6*R*-I^2aa analog **4**. For example, against the 12 bacteria strains examined, relative to the MIC values for GS, those for [(6*S*)-$I^2aa^{4-5,4'-5'}$]GS **2** ranged from half potency in five cases, to 1/4 potency in six cases, down to < 1/8 potency in one case. However, relative to the MIC values for GS, the values for [(6*R*)-$I^2aa^{4-5,4'-5'}$]GS **4** were 1/4 potency in one case and ≤ 1/8 potency for the other 11 strains. The replacement of Orn

Table 5. **Antimicrobial activity (minimal inhibitory concentrations in μg/mL) for GS and I^2aa-GS analogs 2–4**

Microbe	GS	[(6*S*)-I^2aa]GS **2**	[Lys, (6*S*)-I^2aa]GS **3**	[(6*R*)-I^2aa]GS **4**
Gram-positive bacteria				
Staphylococcus aureus SAP0017	3.1	12.5	25	100
Staphylococcus aureus K147	3.1	12.5	12.5	100
Staphylococcus epidermidis C621	3.1	12.5	12.5	50
Bacillus subtilis C626	3.1	25	25	100
Enterococcus faecalis C625	6.2	25	25	>100
Corynebacterium xerosis C875	0.8	3.1	3.1	12.5
Gram-negative bacteria				
Pseudomonas aeruginosa H187	50	>100	>100	>100
Pseudomonas aeruginosa H188	6.2	12.5	12.5	25
Escherichia coli UB1005	25	50	50	>100
Escherichia coli DC2	6.2	25	25	50
Salmonella typhimurium C587	25	50	50	>100
Salmonella typhimurium C610	12.5	50	50	100
Yeast				
Candida albicans CAND105	6.2	12.5	12.5	100

with Lys in analogs **2** and **3** had little consequence on antimicrobial activity, except in one case where the Lys analog **3** was 1/2 as potent as its Orn counterpart **2**. In the antifungal assay, [(6*S*)-$I^2aa^{4-5,4'-5'}$]GS analogs **2** and **3**, both were half as potent as GS against *Candida albicans* and [(6*R*)-$I^2aa^{4-5,4'-5'}$]GS **4** was 1/16 as potent as GS.

The concentration of GS and [$I^2aa^{4-5,4'-5'}$]GS analogs **2–4** required for complete lysis of red blood cells was determined after 4 and 24 h (Table 6) (13). In this assay, [$I^2aa^{4-5,4'-5'}$]GS analogs **2–4** exhibited 4-fold less hemolytic activity than GS after 4 h. Because [(6*S*)-$I^2aa^{4-5,4'-5'}$]GS analogs **2** and **3** exhibited a greater therapeutic index (hemolytic activity/antibiotic activity) than GS against yeast as well as against 5 of the 12 bacteria studied (42%), the anti-eukaryotic and antimicrobial activities of GS were thus dissociated through modification at the peptide turn regions using (3*S*, 6*S*, 9*S*)-indolizidin-2-one amino acid.

Discussion and Conclusion

We have developed solution- and solid-phase methodology for incorporating indolizidin-2-one amino acids into cyclic-peptide structures. Both the concave (3*S*, 6*S*, 9*S*)- and convex (3*S*, 6*R*, 9*S*)-indolizidin-2-one amino acids (6*S*)- and (6*R*)-**1** were introduced at the turn regions of gramicidin S in order to examine the influence of configuration on conformation and antimicrobial activity. The resulting [$I^2aa^{4-5,4'-5'}$]GS analogs **2–4** have been examined using circular dichroism and NMR spectroscopy as well as evaluated for antibacterial, antifungal and hemolytic activities in order to study the influence of turn geometry on the potency and specificity of the native peptide.

The significance of the type II′ β-turn conformation to the antibacterial potency of GS against gram-positive organisms has been illustrated previously by replacement of the D-Phe-Pro residues with different peptide sequences (22, 23, 48, 53–56), as well as with β-turn mimics (27–35). Antibacterial activity against gram-positive bacteria persisted or was decreased slightly by modifications that maintained the type II′ geometry; however, activity was lost when the type II′ β-turn was significantly perturbed. In GS, the type II′ β-turns stabilize an antiparallel β-pleated sheet geometry essential for antibacterial activity by favoring formation of 10- and 14-membered hydrogen-bonds (57, 58). Stabilization of such a sheet structure by an organic nucleator has also led to antibacterial activity in a linear analog (32).

An influence of ring-fusion stereochemistry on the conformation and antibacterial activity of GS was demonstrated previously in analogs possessing 2-amino-3-oxohexahydroindolizino[8,7-*b*]indole-5-carboxylic acid (IBTM, Fig. 1) as a dipeptide surrogate at one of the type II′ β-turn positions (33, 34). The analog [$Lys^{2,2'}$,(*S*)-$IBTM^{4-5}$]GS did not exhibit NMR spectral characteristics (i.e. NOEs, chemical shifts, amide temperature coefficients nor $^3J_{NH\text{-}C\alpha H}$

Table 6. **Antihemolytic activity for GS and I²aa-GS analogs 2-[4a]**

Peptide	4h	24h
GS	100	25
[(6*S*)-I²aa]GS **2**	400	100
[Lys, (6*S*)-I²aa]GS **3**	400	100
[(6*R*)-I²aa]GS **4**	200	100

a. Minimal concentration necessary for 100% cell lysis in μg/mL.

coupling constant values) that were consistent with the preferred conformation of GS. However, the isomeric [Lys$^{2,2'}$, (*R*)-IBTM$^{4-5}$]GS and [(*R*)-IBTM$^{4-5}$]GS, both exhibited NMR spectral data characteristic of the β-turn/antiparallel β-pleated sheet conformation adopted by GS. Against gram-positive bacteria, the [(*R*)-IBTM$^{4-5}$]GS analogs exhibited activity comparable with GS; however, isomeric [Lys$^{2,2'}$,(*S*)-IBTM$^{4-5}$]GS was only 1/32 as potent as GS. In this example, the biologically active mimic possessed an indolizidinone with the ring-fusion proton on the same face as the amine and carboxylate substituents. Although the limited availability of the ring-fusion diastereomer of the thiaindolizidinone amino acid BTD has prevented a comparison of [BTD$^{4-5}$]GS analogs possessing different stereochemistry, potent antibacterial analogs exhibiting similar CD and NMR spectra to that of native GS were generated by the incorporation of BTD with the ring-fusion proton on the same face as the amine and carboxylate substituents (27, 28). The importance of the indolizidinone ring-fusion stereochemistry for effective β-turn mimicry has been considered outside the context of GS. For example, in a computational study, a comparison of BTD with (6*R*)- and (6*S*)-I²aa suggested that the geometry of the turn induced by these indolizidinone analogs differed significantly from ideal β-turns and that the (6*S*)-I²aa was the most effective as a reverse turn mimic (59). More recently, a combination of computational NMR spectroscopic analysis of oxaindolizidinone amino acid **14** (Fig. 1) predicted the isomer possessing the ring-fusion proton on the same face as the amine and carboxylate substituents to be a better mimic of a β-turn geometry than its ring-fusion diastereomer (60).

The effect of indolizidin-2-one configuration on the conformation of GS was studied by comparing the spectral properties of [I²aa$^{4-5,4'-5'}$]GS analogs **2** and **4** possessing the concave (3*S*, 6*S*, 9*S*)- and convex (3*S*, 6*R*, 9*S*)-configurations. Circular dichroism spectroscopy of [I²aa$^{4-5,4'-5'}$]GS analogs **2–4** in solution provided curve shapes similar to GS albeit with weaker band intensity, as was observed in CD spectra of [BTD$^{4-5}$]GS analogs and attributed to removal of the aromatic Phe chromophore. Because the CD spectra of these cyclic peptides results from contributions from the β-turns, aromatic chromophore and β-sheet structure, it is difficult to use this technique to discuss particular secondary structural elements. Nevertheless, the significantly weaker band intensity exhibited by [(6*R*)-I²aa$^{4-5,4'-5'}$]GS **4** relative to its (6*S*)-counterparts **2** and **3** suggests that the (6*R*)-I²aa analog is less proficient in adopting a conformation similar to GS than the (6*S*)-I²aa analog. In the NMR spectra of [I²aa$^{4-5,4'-5'}$]GS analogs **2–4**, all three analogs exhibited NOEs, amide temperature coefficients and $^3J_{\text{NH-C}\alpha\text{H}}$ coupling constant values that supported a β-pleated sheet conformation. Significant differences in the number and intensity of the nonsequential NOEs between the opposing Val and Leu residues did, however, indicate that [(6*S*)-I²aa$^{4-5,4'-5'}$]GS **2** was more proficient in adopting the antiparallel β-pleated sheet conformation relative to its 6*R*-diastereomer **4**. Evaluation of [I²aa$^{4-5,4'-5'}$]GS analogs **2–4** against different microbial strains provided a sensitive means for distinguishing the importance of ring-fusion stereochemistry. In particular, the [(6*S*)-I²aa$^{4-5,4'-5'}$]GS analogs **2** and **3** exhibited antimicrobial activity that was typically 2–8 times greater in potency than isomeric [(6*R*)-I²aa$^{4-5,4'-5'}$]GS (**4**).

Relative to GS, [(6*S*)-I²aa$^{4-5,4'-5'}$]GS (**2**) exhibited 2–4-fold less activity against 11 bacterial strains as well as 2-fold less antifungal activity. Similarly, peptide **2** showed reduced hemolytic activity, 4-fold less than GS. Against certain microbial strains, the antimicrobial and hemolytic activities of GS were thus differentiated by this modification at the peptide turn region.

Besides influencing peptide conformation, substitution of I²aa for the D-Phe-Pro residues removed the aromatic side chains at the turn regions of GS. Replacement of D-phenylalanine by D-cyclohexylalanine and D-alanine in GS caused slight reductions in antibacterial potency (37), indicating that aromatic groups may be removed with little loss in potency as long as the conformation and hydrophobicity at the turn region are retained. In one study, hemolytic activity has been shown to be contingent on the aromatic character at the turn region (11). The reduced activity of peptides **2–4** may thus result in part from removal of the aromatic side chains, which may in certain cases have a more pronounced consequence on hemolytic rather than antimicrobial activity.

The ring fusion configuration of indolizidinone dipeptide surrogates can influence the conformation and activity of peptide analogs possessing azabicyclo[X.Y.0]alkane amino acids. In [I²aa$^{4-5,4'-5'}$]GS analogs, a change in ring fusion stereochemistry from the concave 6*S*- to the convex

6*R*-geometry resulted in subtle differences in the CD and NMR spectral properties of peptides **2–4**, indicating modest conformational differences. Such conformational changes did, however, have a pronounced impact on antimicrobial potency. With respect to the inverse relationship between NOE intensity and distance, the closer proximity of the opposing Val and Leu residues in [(6*S*)-I²aa$^{4-5,4'-5'}$]GS (**2**) may account for its greater potency compared with [(6*R*)-I²aa$^{4-5,4'-5'}$]GS (**4**). A closely packed network of aliphatic side-chains, a hydrophobic wedge, may thus be a requirement for antimicrobial activity in the natural peptide.

Experimental Procedures

General

Unless noted otherwise, all reactions were run under argon atmosphere and distilled solvents were transferred by syringe. Tetrahydrofuran (THF) was distilled from sodium/benzophenone immediately before use, CH_2Cl_2 was distilled from P_2O_5, DMF and acetonitrile were distilled from CaH_2, Et_3N was distilled from BaO, DIEA was distilled first from ninhydrin and then from CaH_2. Final reaction mixture solutions were dried over Na_2SO_4. Melting points are uncorrected. Mass spectral data, HRMS and MS (EI, FAB and MALDI), were obtained by the Université de Montréal mass spectroscopy facility. Analytical thin-layer chromatography (TLC) was performed by using 2 × 6 cm aluminum-backed silica plates coated with a 0.2-mm thickness of silica gel 60 F_{254} (Merck) with UV-light, ninhydrin and iodine as revealing agents. Chromatography was performed using Kieselgel 60 (230–400 mesh). Dowex 50W-X8 H^+ form with 1.9 meq/mL (wet volume) was used as cation exchange resin. Analytical HPLC was performed with a flow rate of 1.5 mL/min and detection at 220 nm on: (i) an inverse-phase column Prep DeltaPak HR C_{18} (6 μm, 60 Å, 8 × 100 mm) with an inverse-phase precolumn Prep NovaPak HR C_{18} (6 μm 60 Å) eluting with a linear gradient of 90:10:0.01 to 0:100:.01 (v/v) H_2O/CH_3CN/TFA over 30 min; and (ii) a Higgins C_{18} Targa column (4.6 × 250 mm, particle size 5 μm, pore size 120 Å) using a gradient of water in acetonitrile containing 0.003 and 0.05% TFA, respectively. Unless stated elsewhere, preparative reversed-phase HPLC was performed on a Waters system with a Higgins C_{18} Targa column (20 × 250 mm, particle size 5 μm, pore size 120 Å) with a 20-mL/min flow rate and a gradient of H_2O (0.05% TFA) to 75% CH_3CN/H_2O (0.008% TFA).

Biological examination of peptides **2–4** and GS in antimicrobial and hemolytic tests was performed according to the protocols described previously (11, 13).

Circular dichroism measurements

CD spectra of 0.1 mM solutions in H_2O and CH_3OH were measured on a Jasco J-710 spectropolarimeter using a circular quartz cell with a path length of 1 mm at 23°C. Spectra were run with a band width of 1 nm, a response time of 0.25 s and a scan speed of 100 nm/min. Each measurement was the average result of 10 repeated scans in steps of 0.2 nm. Baseline spectra of the solvents were subtracted. The Cotton effect was evaluated in terms of molar ellipticity [θ].

NMR measurements

^1H and ^{13}C NMR experiments were performed on Bruker DMX600 and ARX400 spectrometers. The chemical shifts are reported in p.p.m. (δ units) downfield of the internal tetramethylsilane ($(CH_3)_4Si$) or dioxane. Coupling constants are in Hz. COSY, TOCSY and ROESY spectra were obtained on samples in water (9:1 H_2O/D_2O) at pH 6.5 without added buffer at concentrations of ≈ 5 mM. Spectra were measured at 23°C with 2048 by 512 or 1024 data points with mixing times of 105, 73 and 77 ms for the respective TOCSY spectra of **2**, **3** and **4**; 500 ms for NOESY spectra. The intensity of the cross-peaks was measured in the NOESY spectra was ascertained by giving the peak of highest intensity a value of 100% and ranking the other cross-peaks as strong (> 65%), medium (< 65% > 20%) and weak (< 20%).

Boc-(Cbz)Orn-Leu-O-allyl Ester

A solution of N^{α}-(Boc)-N^{δ}-(Cbz)ornithine (Sigma, 733 mg, 2 mmol, 100 mol percentage) in CH_3CN (16 mL) was treated with L-leucine allyl ester *p*-toluenesulfonate (38) (914 mg, 2.2 mmol, 110 mol percentage) followed by Et_3N (0.62 mL, 44 mmol, 220 mol percentage) and TBTU (626 mg, 2.2 mmol, 110 mol percentage), and stirred at room temperature for 12 h when TLC (20:1 EtOAc/AcOH) showed complete consumption of starting material. Brine (50 mL) was added, the mixture was extracted with EtOAc (3 × 15 mL), the combined organic layers were washed with

2 N HCl (2 mL), H_2O (2 mL), 5% $NaHCO_3$ (2 mL) and H_2O (2 mL), dried and evaporated to a solid that was chromatographed with 1:1 EtOAc/hexane as eluant to give a white solid, Boc-(Cbz)Orn-Leu-O-allyl ester (992 mg, 95%): R_f = 0.7 (1:1 EtOAc/hexane); ^{1}H NMR δ 0.82 (m, 6 H), 1.3 (s, 9 H), 1.42–1.65 (m, 6 H), 1.75 (m br, 1 H), 3.04 (m, 1 H), 3.21 (m, 1 H), 4.27 (m, 1 H), 4.48 (m br, 3 H), 4.9 (m, 2 H), 5.15 (m, 2 H), 5.6 (d br, 1 H, *J* = 15.6 Hz), 5.65 (m br, 1 H), 5.7 (m, 1 H), 7.19 (s br, 1 H), 7.2 (s, 5 H); ^{13}C NMR δ 21.3, 22.5, 24.3, 25.5, 27.9, 29.6, 39.5, 40.4, 50.5, 52.7, 65.3, 66.1, 79.1, 118.1, 127.6, 128.0 (2 C), 131.4, 136.3, 155.4, 156.7, 172.0, 172.2.

Boc-Val-(Cbz)Orn-Leu-O-allyl ester

A solution of Boc-(Cbz)Orn-Leu-O-allyl ester (990 mg, 1.90 mmol, 100 mol percentage) in TFA (15 mL) and CH_2Cl_2 (30 mL) was stirred for 30 h at room temperature when TLC (1:1 EtOAc/hexane) showed complete disappearance of starting carbamate and the formation of a ninhydrin positive product at a lower R_f value (R_f = 0.07 using 4:1:1 *n*-BuOH/AcOH/H_2O). The volatiles were removed under vacuum and the trifluoroacetate salt was dissolved in CH_3CN (16 mL), treated with *N*-(Boc)valine (454 mg, 2.09 mmol, 110 mol percentage), Et_3N (0.60 mL, 3.97 mmol, 210 mol percentage) and TBTU (595 mg, 2.09 mmol, 110 mol percentage), and stirred for 12 h at room temperature when TLC (4:1:1 *n*-BuOH/AcOH/H_2O) showed complete consumption of starting material. Brine (50 mL) was added, the mixture was extracted with EtOAc (3 × 15 mL), and the combined organic layers were washed with 2 N HCl (2 mL), H_2O (2 mL), 5% $NaHCO_3$ (2 mL) and H_2O (2 mL), dried and evaporated to a solid that was chromatographed with 2:1 EtOAc/hexane as eluant to give a white solid that recrystallized from Et_2O in hexane. Boc-Val-(Cbz)Orn-Leu-O-allyl ester (826 mg, 70%): R_f = 0.68 (4:1 EtOAc/hexanes); mp 141°C; $[\alpha]_D^{20}$ −8.7° (≈ 1, $CHCl_3$); ^{1}H NMR δ 0.88–0.94 (m, 12 H), 1.42 (s, 9 H), 1.5–1.7 (m, 6 H), 1.82–1.95 (m br, 1 H), 2–2.14 (m, 1 H), 3.08–3.2 (m br, 1 H), 3.3–3.47 (m br, 1 H), 3.95–4.05 (m, 1 H), 4.50–4.55 (m, 1 H), 4.55–4.62 (m, 2 H), 4.62–4.74 (m br, 1 H), 5.08 (dd, 2 H), 5.18–5.35 (dd, 2 H), 5.29 (d br, 1 H), 5.8–5.95 (m br, 1 H), 6.95 (d br, 1 H), 7.15 (d br, 1 H), 7.2 (s, 5 H); ^{13}C NMR δ 17.7, 19.2, 21.6, 22.8, 24.7, 26.1, 28.3, 29.8, 31.0, 39.6, 40.8, 50.9, 51.6, 59.8, 65.7, 66.6, 79.8, 118.6, 128.0, 128.4 (2 C), 131.6, 136.5, 155.8, 157.1, 171.6, 171.9, 172.3; HRMS calcd for $C_{32}H_{51}N_4O_8$ (MH^+) 619.3706, found 619.3731.

Val-(Cbz)Orn-Leu-O-allyl ester trifluoroacetate (5)

Boc-Val-(Cbz)Orn-Leu-O-allyl ester (235 mg, 0.380 mmol) was deprotected using the protocol for Boc group removal described above. Val-(Cbz)Orn-Leu-O-allyl ester trifluoroacetate (**5**, 150 mg, 98%): R_f = 0.07 (4:1:1 *n*-BuOH/AcOH/H_2O); ^{1}H NMR δ 0.85 (m, 6 H), 0.95 (m, 6 H), 1.5–1.7 (m, 6 H), 1.7–1.8 (m br, 1 H), 2.1–2.3 (m, 1 H), 3–3.2 (s br, 2 H), 3.9–4.0 (s br, 1 H), 4.45–4.55 (m, 3 H), 4.70 (s br, 1 H), 5.05 (s br, 2 H), 5.2–5.4 (dd, 2 H), 5.4 (d br, 1 H), 5.8–5.9 (m, 1 H), 7.3 (s, 5 H), 6.95 (d br, 1 H), 7.15 (d br, 1 H); HRMS calcd for $C_{27}H_{43}N_4O_6$ (MH^+) 519.3182, found 519.3180.

Boc-(6*S*)-I^{2}aa-Val-(Cbz)Orn-Leu-O-allyl ester (6)

Trifluoroacetate **5** (237 mg, 0.380 mmol, 103 mol percentage) and (3*S*, 6*S*, 9*S*)-2-oxo-3-*N*-(Boc)amino-1-azabicyclo [4.3.0]nonane-9-carboxylic acid ((3*S*, 6*S*, 9*S*)-**1**, 110.3 mg, 0.370 mmol, 100 mol percentage) were coupled using the procedure described above. Chromatography with 1:5 hexane/EtOAc as eluant gave a white solid that recrystallized from Et_2O/hexane. Boc-(6*S*)-I^{2}aa-Val-(Cbz)Orn-Leu-O-allyl ester (**6**, 249 mg, 84%): R_f = 0.41 (EtOAc); mp 91–92°C; $[\alpha]_D^{20}$ −36.9° (≈ 1, $CHCl_3$); ^{1}H NMR δ 0.84–0.88 (m, 12 H), 1.37 (s, 9 H), 1.45–1.7 (m, 8 H), 1.77–1.9 (m, 2 H), 2–2.15 (m, 4 H), 2.2–2.3 (m, 2H), 3.1 (m br, 1 H), 3.3 (m br, 1 H), 3.55 (m, 1 H), 3.95 (m, 1 H), 4.15 (dd, 1 H), 4.45–4.52 (m, 3 H), 4.56 (m, 2 H), 5.0 (dd, 2 H), 5.2 (dd, 2 H), 5.35 (s br, 1 H), 5.35 (d, 1 H), 5.8 (m br, 1 H), 6.9 (d br, 2 H), 7.2–7.3 (m, 6 H); ^{13}C NMR δ 17.9, 19.3, 21.5, 22.7, 24.6, 25.7, 26.6, 27.5, 28.2, 28.3, 29.2, 30.2, 32.2, 39.9, 40.5, 49.7, 50.8, 52.1, 57.4, 58.7, 59.8, 65.5, 66.4, 79.6, 118.3, 127.9, 128.2, 128.3, 131.7, 136.5, 155.6, 156.8, 170.3, 171.0, 171.2, 171.5, 172.2; HRMS calcd for $C_{41}H_{63}N_6O_{10}$ (MH^+) 799.4607, found 799.4573.

Boc-(6*S*)-I^{2}aa-Val-(Cbz)Orn-Leu (7)

A solution of allyl ester **6** (60 mg, 0.075 mmol) in THF (1.3 mL) was treated with $Pd(PPh_3)_4$ (8.7 mg, 0.0075 mmol, 10 mol%) and morpholine (65 μL, 0.75 mmol, 1000 mol%) then stirred for 4 h when TLC (20:1 EtOAc/AcOH) showed complete disappearance of **6**. The solvent was evaporated, the residue was taken up in 2.4 mL of CH_2Cl_2 and washed with 2 N HCl (3 × 2.4 mL), dried and evaporated to a solid that was chromatographed with 1:5 isopropanol/$CHCl_3$ as

eluant to give Boc-I²aa-Val-(Cbz)Orn-Leu (**5**, 54 mg, 95%) as a white solid (on larger scale, 135 mg of **6** yielded 76% of **7**): R_f = 0.27 (3:1 $CHCl_3$/isopropanol); R_f = 0.24 (1:1 EtOAc/MeOH); ^{1}H NMR (CD_3OD) δ 0.89–0.98 (m, 12 H), 1.44 (s, 9 H), 1.52–1.72 (m, 8 H), 1.74–1.89 (m br, 2 H), 1.98–2.18 (m, 6 H), 3.08–3.20 (m br, 2 H), 3.66 (m br, 1 H), 4.07–4.15 (m, 2 H), 4.37 (m, 1 H), 4.42–4.48 (m br, 1 H), 5.06 (m, 2 H), 7.29–7.3; ^{13}C NMR (CD_3OD) δ 19.2, 20.1, 22.1, 23.8, 26.1, 27.0, 27.3, 28.9, 29.4, 30.2, 30.5, 31.9, 33.0, 41.4, 42.4, 50.7, 53.7, 54.3, 60.3, 60.7, 61.0, 67.6, 80.7, 129.0, 129.1, 129.6, 138.5, 158.1, 159.0, 171.0, 173.6 (2 C), 174.4, 179.0; HRMS calcd for $C_{38}H_{59}N_6O_{10}$ (MH^+) 759.4293, found 759.4322.

(6*S*)-I²aa-Val-(Cbz)Orn-Leu-O-allyl ester trifluoroacetate (8)

A solution of Boc-(6*S*)-I²aa-Val-(Cbz)Orn-Leu-O-allyl ester (**6**, 124 mg, 0.155 mmol) in CH_2Cl_2 (6 mL) was treated with TFA (1.5 mL) at 25°C and stirred for 15 h when TLC (4:1 EtOAc/hexanes) showed complete disappearance of starting material and the formation of a new ninhydrin positive product at a lower R_f value (R_f = 0.07). The volatiles were evaporated and the salt was used directly in the next reaction. (6*S*)-I²aa-Val-(Cbz)Orn-Leu-O-allyl ester trifluoroacetate (**8**, 123 mg, 98%): R_f = 0.07 (4:1:1 *n*-BuOH/AcOH/H_2O); ^{1}H NMR (CD_3OD) δ 0.88–0.97 (m, 12 H), 1.66–1.74 (m, 8 H), 1.78–1.95 (m, 2 H), 2.04–2.19 (m, 5 H), 2.34 (m, 1H), 3.10–3.21 (m, 2 H), 3.72 (m, 1 H), 3.94 (t, 1 H, J = 8.1), 4.18 (m, 1 H), 4.45–4.62 (m, 5 H), 5.06 (m, 2 H), 5.21 (dd, 1 H, J = 1.3, 10.5), 5.30 (dd, 1 H, J = 1.5, 17.2), 5.90 (m, 1 H), 7.27–7.32 (m, 5 H); ^{13}C NMR (CD_3OD) δ 18.9, 19.9, 21.9, 23.4, 25.6, 25.9, 26.9, 27.1, 30.57, 30.64, 32.2, 32.9, 41.2, 41.5, 49.8, 52.2, 53.7, 59.2, 60.4, 60.9, 66.9, 67.5, 119.0, 128.9, 129.1, 129.6, 133.3, 138.4, 159.0, 167.2, 173.4, 173.7(2 C), 174.0; HRMS calcd for $C_{36}H_{55}N_6O_8$ (MH^+) 699.4081, found 699.4101.

Boc-(6*S*)-I²aa-Val-(Cbz)Orn-Leu-(6*S*)-I²aa-Val-(Cbz)Orn-Leu-O-allyl ester (9)

Trifluoroacetate **8** (123 mg, 0.151 mmol, 120 mol%) in CH_3CN (1.5 mL) was treated with Boc-(6*S*)-I²aa-Val-(Cbz)Orn-Leu (**7**, 96 mg, 0.127 mmol, 100 mol percentage) followed by TBTU (49.4 mg, 0.152 mmol, 120 mol percentage) and Et_3N (40 μL, 0.279 mmol, 220 mol percentage), and stirred at room temperature for 12 h. Brine (2 mL) was added, the mixture was extracted with EtOAc (3 × 2 mL), and the combined organic layers were washed with 2 N HCl (0.2 mL), H_2O (0.2 mL), 5% $NaHCO_3$ (0.2 mL) and H_2O (0.2 mL), dried and evaporated to a solid that was chromatographed with a gradient of 0–10% MeOH in EtOAc as eluant to give Boc-(6*S*)-I²aa-Val-(Cbz)Orn-Leu-(6*S*)-I²aa-Val-(Cbz)Orn-Leu-*O*-allyl ester (**9**, 158 mg, 87%) as a white solid: R_f = 0.67 (5:1 EtOAc/AcOH); mp 142–143°C; $[\alpha]_D^{20}$ −50.5° (≈ 1, $CHCl_3$); ^{1}H NMR δ 0.8–1.05 (m, 24 H), 1.32 (s, 9 H), 1.5–1.8 (m, 16 H), 1.8–1.95 (m, 4 H), 2.0–2.2 (m, 8 H), 2.25–2.4 (m, 4H), 3–3.25 (m, 4 H), 3.45–3.68 (m, 3 H), 3.81 (m, 1 H), 3.95 (m, 1 H), 4.05 (m, 1 H), 4.15–4.38 (m, 5 H), 4.5 (m, 1 H), 4.55–4.6 (m, 2 H), 4.90–4.99 (dd, 2 H), 5.01–5.08 (dd, 2 H), 5.11 (dd, 1 H), 5.24 (dd, 1 H), 5.68 (s br, 1 H), 5.90 (s br, 1 H), 5.90 (m, 1 H), 6.1 (s br, 1 H), 6.5–8.0 (s, 7 H), 7.2–7.4 (m, 10 H); ^{13}C NMR δ 19.2, 19.5, 20.1, 20.7, 21.0, 21.6, 22.9, 23.0, 24.3, 24.7, 25.0, 25.4, 25.6, 26.4, 27.0, 27.6, 28.3, 28.5, 29.2 (2 C), 29.6, 30.6, 31.4, 31.8, 32.0, 39.7, 40.3, 40.6, 41.1, 48.7, 50.8 (2 C), 52.7, 53.8, 54.5, 59.6, 60.3, 60.8 (2 C), 61.6, 62.9, 65.5, 66.4, 66.6, 79.9, 117.9, 127.5, 127.8, 127.9, 128.3 (2 C), 128.5, 132.1, 136.5, 136.9, 155.9, 156.3, 156.6, 169.0, 170.1, 171.3, 171.7, 172.2, 172.4, 172.7, 173.1, 173.4, 173.6; MS calcd for $C_{74}H_{110}N_{12}O_{17}$ (M) 1439.77, found (M^+) 1439.9.

(6*S*)-I²aa-Val-(Cbz)Orn-Leu-(6*S*)-I²aa-Val-(Cbz)Orn-Leu trifluoroacetate (10)

A solution of protected peptide **9** (158 mg, 0.11 mmol) in THF (1.9 mL) was treated with $Pd(PPh_3)_4$ (12.7 mg, 0.011 mmol, 10% mol) and morpholine (96 μL, 1.10 mmol, 1000 mol%), and stirred for 4 h when TLC (5:1 EtOAc/MeOH) showed complete disappearance of ester **9**. The solvent was evaporated, the residue was taken up in 3 mL of CH_2Cl_2, extracted three times with 2 mL of 2 N HCl, dried and evaporated to a solid, that was filtered through a plug silica gel. Boc-(6*S*)-I²aa-Val-(Cbz)-Orn-Leu-(6*S*)-I²aa-Val-(Cbz)Orn-Leu (101 mg, 66%): R_f = 0.56 (20:1 EtOAc/AcOH); retention time (RT) = 24.2 min; ^{1}H NMR (CD_3OD) δ 0.8–1.05 (m, 24 H), 1.32 (s, 9 H), 1.5–1.8 (m, 16 H), 1.8–1.95 (m, 4 H), 2–2.2 (m, 8 H), 2.25–2.4 (m, 4 H), 3–3.25 (m, 4 H), 3.45–3.68 (m, 3 H), 3.81 (m, 1 H), 3.95 (m, 1 H), 4.05 (m, 1 H), 4.15–4.38 (m, 5 H), 4.5 (m, 1 H), 4.90–4.99 (dd, 2 H), 5.01–5.08 (dd, 2 H), 7.2–7.4 (m, 10 H); MS calcd for $C_{71}H_{106}N_{12}O_{17}$ (M) 1399.71, found (M^+) 1399.3.

A solution of Boc-(6*S*)-I²aa-Val-(Cbz)Orn-Leu-(6*S*)-I²aa-Val-(Cbz)Orn-Leu (96 mg) in CH_2Cl_2 (5 mL) was treated with TFA (1 mL) at 25°C and stirred for 15 h when TLC

(20:1 EtOAc/AcOH) showed complete disappearance of starting material and the formation of a new ninhydrin positive product at a lower R_f value ($R_f = 0.47$, 4:1:1 *n*-BuOH/AcOH/H_2O). The volatiles were evaporated yielding trifluoroacetate salt **10**. Analysis by HPLC showed complete consumption of the Boc-derivative (RT = 22.2 min) and appearance of a new peak for **10** at RT = 19.3 min (6*S*)-I²aa-Val-(Cbz)Orn-Leu-(6*S*)-I²aa-Val-(Cbz)Orn-Leu trifluoroacetate salt (**10**, 92 mg, 95%): $R_f = 0.47$ (4:1:1 *n*-BuOH/AcOH/H_2O); ^{1}H NMR (CD_3OD) δ 0.8–1.05 (m, 24 H), 1.5–1.8 (m, 16 H), 1.8–1.95 (m, 4 H), 2–2.2 (m, 8 H), 2.25–2.4 (m, 4H), 3–3.25 (m, 4 H), 3.45–3.68 (m, 3 H), 3.81 (m, 1 H), 3.95 (m, 1 H), 4.05 (m, 1 H), 4.15–4.38 (m, 5 H), 4.5 (m, 1 H), 4.90–4.99 (dd, 2 H), 5.01–5.08 (dd, 2 H), 7.2–7.4 (m, 10 H); ^{13}C NMR δ 20.5, 20.7, 21.6 (2 C), 23.5, 23.8, 25.2 (2 C), 27.5, 27.3, 27.6 (2 C), 28.8 (4 C), 30.5, 31.9, 32.2 (2 C), 33.7, 33.8, 32.4, 34.5, 42.9 (2 C), 43.4, 43.8, 53.6 (2 C), 54.8 (2 C), 55.5 (2 C), 60.8 (2 C), 62.1 (2 C), 62.5 (2 C), 69.0 (2 C), 130.5, 130.6, 130.7, 131.2 (2 C), 131.6, 131.7, 134.7, 134.8, 135.5, 133.9, 140.1, 160.5 (2 C), 168.8, 172.8, 174.9, 175.0, 175.3, 175.4, 175.5, 175.6, 175.7, 177.5; MS calcd for $C_{66}H_{98}N_{12}O_{15}$ (M) 1299.6, found (MH^+) 1300.6.

Cyclo((6*S*)-I²aa-Val-(Cbz)Orn-Leu)$_2$ (11)

A solution of trifluoroacetate salt **10** (92 mg, 0.065 mmol, 100 mol%) in DMF (43.3 mL, $\approx 1 \times 10^{-3}$ M) was treated with TBTU (62.4 mg, 0.195 mmol, 300 mol percentage) and 1-hydroxybenzotriazole hydrate (HOBt, 26.2 mg, 0.195 mmol, 300 mol percentage) at room temperature. After a vigorous agitation, diisopropylethylamine (68 µL, 0.390 mmol, 600 mol%) was added and the mixture was stirred for 1 h when HPLC showed complete disappearance of starting material (**10**, RT = 19.3 min). After concentration of the volatiles, brine (8 mL) was added and the mixture was extracted with EtOAc (3 × 8 mL). The combined organic layers were washed successively with 2 N HCl (0.8 mL), H_2O (0.8 mL), 5% $NaHCO_3$ (0.8 mL) and H_2O (0.8 mL), dried and evaporated to a solid (72 mg, 85%). Purification by HPLC on a preparative inverse phase Watman column C_{18} (10 µm, 100 Å, 22 × 500 mn) eluting with a linear gradient of 60:40:0.01 to 0:100:0.01 (v/v/v) H_2O/CH_3CN/TFA over 60 min with a flow rate of 20 mL/min and detection at 220 nm, followed by lyophylization of the appropriate fractions afforded the cyclic decapeptide, *cyclo*-(6*S*)-I²aa-Val-(Cbz)Orn-Leu)$_2$ (**11**, 50.2 mg, 60%): RT = 27.5 min; mp 182–183°C; $[\alpha]_D^{20}$ +201.3° (≈ 1, $CHCl_3$); ^{1}H NMR (C2 symmetry) δ 0.75–0.76 (m, 18 H), 0.83 (d, 3 H, *J* = 5.7 Hz), 1.32–1.50 (m, 7 H), 1.72–1.77 (m, 1 H), 1.82–1.91 (m, 4 H), 1.99–2.06 (m, 3 H), 2.18 (m, 1H), 2.89 (m, 1 H), 3.02 (m, 1 H), 3.26 (m, 1 H), 3.41 (d, 1 H, *J* = 7.2), 3.89 (dd, 1 H, *J* = 9), 4.29–4.34 (m, 2 H), 4.75 (m, 1 H), 4.94 (ddd, 2 H, *J* = 11, 11, 12), 4.97 (s, 1 H), 7.12–7.23 (m, 5 H), 7.6–7.67 (m, 2 H), 8.23 (d, 1 H), 8.64 (d, 1 H); ^{13}C NMR (C2 symmetry) δ 19.1, 19.4, 22.7, 22.8, 24.7, 25.1, 27.2, 29.4, 29.6, 29.9, 30.4, 31.1, 40.7, 41.4, 48.7, 50.7, 52.1, 59.5, 60.7, 61.0, 66.1, 127.5, 127.9, 128.2, 137.1, 156.9, 168.0, 170.8, 171.5, 171.7, 171.9; MS calcd for $C_{66}H_{96}N_{12}O_{14}$ (M) 1281.6, found (M) 1281.3 and (MH^+) 1282.6.

Cyclo((6*S*)-I²aa-Val-Orn-Leu)$_2$ ([(6*S*)-I²aa$^{4-5,4'-5'}$]GS, 2 (35)

A solution of *cyclo*-(6*S*)-I²aa-Val-(Cbz)Orn-Leu)$_2$ (**11**, 13.4 mg, 0.0104 mmol) in 90% aq. MeOH (6.8 mL) was treated with 1 M HCl (30 µL) and palladium black (1.4 mg, 10% by wt.), and stirred under 1 atm of hydrogen for 15 h. The catalyst was removed by filtration on Celite™ and the filtrate was concentrated under vacuum. Mass spectral analysis showed that only one Cbz group was removed (MS calcd for $C_{58}H_{90}N_{12}O_{12}$ (MH^+) 1147.43, found 1148.0). The residue and fresh catalyst were resubjected to the same hydrogenation conditions for 12 h. Filtration, evaporation of the volatiles and purification by HPLC on a preparative inverse-phase column NovaPak HR C_{18} (6 µm, 60 Å, 25 × 100 mm) equipped with a Prep NovaPak HR C_{18} precolumn (6 µm 60 Å) eluting with a linear gradient of 90:10:0.01 to 0:100:0.01 (v/v/v) H_2O/CH_3CN/TFA over 30 min with a flow rate of 10 mL/min and detection at 220 nm afforded *cyclo*-(6*S*)-I²aa-Val-Orn-Leu)$_2$ ([(6*S*)-I²aa$^{4-5,4'-5'}$]GS, **2**, 11 mg, 98%) as a white hydrochloride salt: $R_f = 0.82$ (4:1:1 *n*-BuOH/AcOH/H_2O); RT = 18.2 min; mp 283–285 dec.°C; $[\alpha]_D^{20}$ −199.4° (≈ 1, CH_3OH); ^{1}H NMR (CD_3OD, C2 symmetry) δ 0,95 (m, 9 H, γ Val, δ Leu), 1.04 (m, 3 H, γ Val), 1.58 (m, 3 H, β Leu, γ Leu), 1.76 (m, 4 H, I²aa 7, γ Orn, β Orn), 2.0 (m, 3 H, β Orn, I²aa 4, 5), 2.16 (m, 2 H, I²aa 8,5), 2.3–2.4 (m, 4 H, I²aa 7, 8, 4, β Val), 3.05 (m, 2 H, δ Orn), 3.78 (m, 1 H, I²aa 6), 3.99 (t, 1 H, I²aa 3), 4.21 (t, 1 H, α Val), 4.5 (m, 1 H, I²aa 9), 4.6 (m, 1 H, α Leu), 7.95 (d, 1 H, NH Val), 8.5 (d, 1 H, NH Orn), 8.7 (d, 1 H, NH Leu), 8.9 (d, 1 H, NH I²aa); ^{13}C NMR (CD_3OD, C2 symmetry) δ 19.9, 20.1, 23.3 (2 C), 24.5, 26.1, 28.3 (2 C), 30.9 (2 C), 31.5, 32.4, 40.5, 42.5, 50.2, 52.1, 52.3, 61.5, 62.7, 62.8, 170.6, 172.6, 172.9, 173.0, 174.7; MS calcd for $C_{50}H_{84}N_{12}O_{10}$ (M) 1013.3, found (M^+) 1013.7 and (MH^+) 1014.2.

Preparation of Boc-Leu-oxime resin and determination of resin loading by synthesis of *N*-(Boc)-leucine *N′-n*-propylamide

Oxime resin (6 g, 0.75 mmol/g, 4.5 mmol) was swollen in CH_2Cl_2 (75 mL), treated with Boc-Leu-OH (5.28 mmol), EACNOx (10.56 mmol) and DCC (5.28 mmol), stirred mechanically overnight, filtered and washed with the following solvent systems: CH_2Cl_2 (3 × 75 mL), 1:1 CH_2Cl_2/EtOH (3 × 75 mL) and CH_2Cl_2 (3 × 75 mL). The resin was then dried under reduced pressure. PA-FTIR spectrum: N-H stretch: 3417 cm^{-1}, ester C = O stretch: 1775 cm^{-1}, carbamate O-(C=O)-N stretch: 1718 cm^{-1}. Two aliquots of Boc-Leu-oxime resin were dried under reduced pressure in joint fitted tubes, weighed (104 and 100 mg), swollen in $CHCl_3$ (2 mL), treated with propylamine (15 μL, 0.18 mmol) and stirred mechanically for 43 h. The resins were each filtered and washed with 2 mL of each of the following solvent systems: $CHCl_3$, 1:1 $CHCl_3$/MeOH and $CHCl_3$. Resin substitution was calculated to be 0.7 mmol/g by weighing the amount of *N*-(Boc)-leucine *N′-n*-propylamide obtained after combination of the filtrates and evaporation: 20 mg and 21 mg; ^{1}H NMR ($CDCl_3$) δ 0.86 (m, 9H), 1.37 (s, 9H), 1.44 (m, 3H), 1.58 (m, 2H), 3.13 (q, J = 7 Hz, 2H), 4.00 (s br, 1H), 4.92 (s br, 1H), 6.24 (s br, 1H). Residual hydroxyl substituents were capped by treating the Boc-Leu-oxime resin (0.687 g, 0.48 mmol) swollen in CH_2Cl_2 (5 mL) with a solution of Ac_2O (0.23 mL, 2.4 mmol) and DIEA (0.17 mL, 0.96 mmol) in CH_2Cl_2 (5 mL), and stirring with a mechanical shaker for 1 h. The resin was finally filtered and washed with CH_2Cl_2 (5 × 10 mL) prior to use in peptide synthesis.

Solid-phase peptide synthesis of linear peptides on oxime resin

Couplings were performed in modified Schlenk tubes possessing a cintered glass filter and two robinets. Removal of the Boc group was achieved by swelling the Boc-Leu-oxime resin (0.687 g) in CH_2Cl_2 (1 mL), stirring mechanically with a 1:3 TFA/CH_2Cl_2 solution (10 mL) for 2 min, filtering and treating again twice for 15 min with a 1:3 TFA/CH_2Cl_2 solution, washing with CH_2Cl_2 (5 × 10 mL) and filtering. The resin was treated with a 1:9 DIEA/CH_2Cl_2 solution (10 mL) and stirred mechanically for 2 min to liberate the free amine. After, the resin was washed with CH_2Cl_2 (3 × 10 mL), it was swollen in DMF (5 mL) and treated with a DMF solution containing the Boc amino acid (200 mol% relative to the resin's substitution, except for Boc-I^{2}aa-OH of which 110 mol% was employed with relative amounts of the other reagents), TBTU (200 mol%) and DIEA (400 mol%). After being stirred mechanically for 2 h, the resin was filtered and washed with DMF (5 × 10 mL) and CH_2Cl_2 (5 × 10 mL). The qualitative ninhydrin test of Kaiser *et al*. (61) was performed on an aliquot of the resin to determine the efficiency of the couplings. When the test was negative, the resin was acetylated using Ac_2O (0.23 mL, 2.4 mmol) and DIEA (0.17 mL, 0.96 mmol) in CH_2Cl_2 for 1 h, washed with CH_2Cl_2 (5 × 10 mL) and the coupling sequence was continued. In the case of a positive test, a second coupling was effected using the same conditions and the resin was then treated with acetic anhydride as described above and washed with CH_2Cl_2 (5 × 10 mL).

Cyclo(Val-Lys(Z)-Leu-(6*S*)-I^{2}aa)$_2$

A suspension of Boc-(6*S*)-I^{2}aa-Val-Lys(Z)-Leu-(6*S*)-I^{2}aa-Val-Lys(Z)-Leu-oxime resin (750 mg, 0.32 mmol/g loading) swollen in CH_2Cl_2 (1 mL) was stirred mechanically with a 1:3 TFA/CH_2Cl_2 solution (10 mL) for 2 min, filtered and treated twice for 15 min with a 1:3 TFA/CH_2Cl_2 solution. The resin was washed with CH_2Cl_2 (5 × 10 mL) and stirred mechanically with a 1:9 DIEA/CH_2Cl_2 solution (10 mL) for 2 min. After being washed with CH_2Cl_2 (3 × 10 mL), the resin was swollen in DMF (5 mL) and stirred mechanically with a solution of DIEA (0.09 mL, 0.5 mmol) and AcOH (0.03 mL, 0.5 mmol) in DMF (5 mL) for 23 h. The resin was filtered, washed with DMF (2 × 10 mL), isopropanol (1 × 10 mL) and DMF (2 × 10 mL), and the combined filtrates were evaporated to a residue that was triturated with water. The residue obtained was purified by flash-column chromatography using 18:1:1 CH_2Cl_2/MeOH/AcOH as eluant. Evaporation of the collected fractions gave 29 mg of cyclo(Val-Lys(Z)-Leu-(6*S*)-I^{2}aa)$_2$ (10% yield, based on initial substitution of the resin). ^{1}H NMR ($CDCl_3$) δ 0.9 (m, 12H), 1.2–2.4 (m, 22H), 2.9 (m, 1H), 3.3 (m, 2H), 3.9 (m, 1H), 4.4 (m, 2H), 5.1 (m, 2H), 7.0 (m, 1H), 7.3 (m, 5H), 7.5 (d, J = 8.7 Hz, 1H), 8.5 (d, J = 9.5 Hz, 1H). Calcd mass for $C_{68}H_{100}N_{12}O_{14}$: 1308.75. MALDI-MS *m/z*: 1310.2 $(M+H)^+$, 1332.3 $(M+Na)^+$, 1348.3 $(M+K)^+$.

Cyclo(Val-Orn(Z)-Leu-(6*R*)-I^{2}aa)$_2$

A suspension of Boc-(6*R*)-I^{2}aa-Val-Orn(Z)-Leu-(6*R*)-I^{2}aa-Val-Orn(Z)-Leu-oxime resin (1.4 g, 0.3 mmol/g loading) swollen in CH_2Cl_2 (1 mL), was treated under the conditions

described above for Boc group removal. After washing with CH_2Cl_2 (4 × 10 mL), the resin was swollen in CH_2Cl_2 (5 mL) and stirred mechanically with a solution of DIEA (0.09 mL, 0.5 mol) and AcOH (0.03 mL, 0.5 mmol) in CH_2Cl_2 (5 mL) for 66 h. The resin was filtered, washed with CH_2Cl_2 (2 × 10 mL), MeOH (1 × 10 mL), CH_2Cl_2 (2 × 10 mL) and MeOH (1 × 10 mL), and the combined filtrates were evaporated, dissolved in a 3:2 MeOH/H_2O solution (2 mL) and eluted through a cation exchange resin to remove DIEA using 3:2 MeOH/H_2O as eluant. The selected fractions were evaporated to give a white solid that was purified using reversed-phase HPLC. Evaporation of the pure fractions yielded 11.4 mg of a white solid (2% yield, based on initial substitution of the resin). ^{1}H NMR ($CDCl_3$) δ 0.9 (m, 12H), 1.25 (m, 8H), 1.55 (m, 6H), 1.8–2.5 (m, 14H), 3.1 (m, 1H), 3.7 (m, 1H), 4.6 (m, 1H), 5.0 (m, 2H), 7.35 (m, 1H), 7.65 (m, 1H), 8.6 (m, 1H). Calcd mass for $C_{66}H_{96}N_{12}O_{14}$: 1280.72. FAB-MS *m/z* 1281.8 $(M+H)^+$.

Cyclo(Val-Lys-Leu-(6*S*)-I^{2}aa)$_2$ (3)

A solution of cyclo(Val-Lys(Z)-Leu-(6*S*)-I^{2}aa)$_2$ (20 mg, 0.015 mmol) in 19:1 MeOH/H_2O (10 mL) was treated with HCl (2 N, 45 μL, 0.09 mmol) and palladium black (2 mg, 0002 mmol). The round-bottomed flask equipped with a balloon was filled, vented and refilled with hydrogen three times, and the suspension was stirred under hydrogen at room temperature for 18 h. The catalyst was filtered onto Celite™ and washed with MeOH (10 mL). The filtrate was concentrated *in vacuo* and the residue obtained was purified by reversed-phase HPLC. Evaporation of the pure fractions yielded 15.5 mg (98%) of a white solid. ^{1}H NMR (H_2O/D_2O 9:1) δ 0.9 (m, 12 H, γ Val, δ Leu), 1.3 (m, 2 H, γ Lys), 1.4 (m, 1 H, γ Leu), 1.52 (m, 2 H, β Leu), 1.6 (m, 4 H, β Lys, δ Lys), 1.7–1.8 (m, 2 H, I^{2}aa 5, β Lys), 1.9 (m, 1 H, I^{2}aa 4), 2.05 (m, 1 H, I^{2}aa 8), 2.1 (m, 2 H, β Val, I^{2}aa 5), 2.15–2.25 (m, 3 H, I^{2}aa 7, 4, 8), 2.9 (m, 2 H, ε Lys), 3.65 (m, 1 H, I^{2}aa 6), 4.05 (m, 2 H, I^{2}aa 3, α Val), 4.35 (m, 2 H, α Leu, I^{2}aa 9), 4.45 (m, 1 H, α Lys), 7.65 (m, 1 H, NH Val), 8.2 (m, 1 H, NH Lys), 8.3 (m, 1 H, NH Leu), 8.65 (m, 1 H, NH I^{2}aa). Calcd mass for $C_{52}H_{88}N_{12}O_{10}$: 1040.67. MALDI-MS *m/z*: 1041.4 $(M+H)^+$, 1063.3 $(M+Na)^+$.

Cyclo(Val-Orn-Leu-(6*R*)-I^{2}aa)$_2$ (4)

A solution of cyclo(Val-Orn(Z)-Leu-(6*R*)-I^{2}aa)$_2$ (11.4 mg, 0.0089 mmol) in 19:1 MeOH/H_2O (5 mL) was treated with HCl (2 N, 25 μL, 0.05 mmol) and palladium black (1.2 mg, 0.0011 mmol) using the conditions described above. Evaporation of the pure HPLC fractions yielded 8.8 mg (98%) of a white solid. ^{1}H NMR (H_2O/D_2O 9:1) δ 0.8 (m, 9 H, γ Val, δ Leu), 0.9 (d, $J = 6.8$ Hz, 3 H, γ Val), 1.4 (m, 3 H, β Leu, γ Leu, I^{2}aa 5), 1.5 (m, 2 H, β Leu, I^{2}aa 7), 1.6 (m, 3 H, β Orn, γ Orn), 1.75 (m, 1 H, I^{2}aa 8), 1.85 (m, 1 H, β Orn), 1.95 (m, 1 H, I^{2}aa 4), 2.15 (m, 4 H, β Val, I^{2}aa 4, 7, 5), 2,5 (m, 1 H, I^{2}aa 8), 2.9 (m, 2 H, δ Orn), 3.7 (m, 2 H, I^{2}aa 3, 6), 4.1 (t, $J = 9$ Hz, 1 H, α Val), 4.5 (m, 2 H, I^{2}aa 9, α Leu), 4.8 (m, 1 H, α Orn), 7.8 (d, $J = 9.3$ Hz, 1 H, NH Val), 8.4 (d, $J = 9.1$ Hz, 1 H, NH Orn), 8.7 (d, $J = 9.4$ Hz, 1 H, NH Leu), 9.0 (d, $J = 6.8$ Hz, 1 H, NH I^{2}aa). Calcd mass for $C_{50}H_{84}N_{12}O_{10}$: 1012.64. FAB-MS *m/z*: 1013.7 $(M+H)^+$.

Acknowledgements: This research was supported in part by the Natural Sciences and Engineering Research Council of Canada, and the Ministère de l'Éducation du Québec. Research by S.W.F. and R.E.W.H. was supported by the Canadian Bacterial Diseases Network. We thank Ms. Sylvie Bilodeau and Dr M. T. Phan Viet of the Regional High-Field NMR Laboratory for assistance with NMR experiments. We thank Dr Marc-André Poupart, Mr Gulian Fazal and Boehringer Ingelheim Canada (Ltée) for assistance with the HPLC purification of **11**. We thank Professor J. Turnbull for use of the CD spectrometer.

References

1. Kotra, L.P., Samama, J.-P. & Mobashery, S. (2001) *Bacterial Resistance to Antimicrobials: Mechanisms, Genetics, Medical Practice and Public Health* (eds Lewis, A., Salyers, A., Haber, H., Wax, R.G.). Decker, New York, pp. 123–159.
2. Garrett, L. (1995) Revenge of the germs, or just keep inventing new drugs. In *The Coming Plague Newly Emerging Diseases in a World Out of Balance*. Penguin Books, New York.
3. Jaynes, B.H., Dirlam, J.P. & Hecker, S.J. (1996) Antibacterial agents. *Ann. Report Med. Chem.* **31**, 121–130.
4. Chu, D.T.W., Plattner, J.J. & Katz, L. (1996) New directions in antibacterial research. *J. Med. Chem.* **39**, 3853–3874.

5. Onishi, H.R., Pelak, B.A., Gerckens, L.S., Silver, L.L., Kahan, F.M., Chen, M.-H., Patchett, A.A., Galloway, S.M., Hyland, S.A., Anderson, M.S. & Raetz, C.R.H. (1996) Antibacterial agents that inhibit lipid A biosynthesis. *Science* **274**, 980–982.
6. Sundram, U.N., Griffin, J.H. & Nicas, T.I. (1996) Novel vancomycin dimers with activity against vancomycin-resistant enterococci. *J. Am. Chem. Soc.* **118**, 13107–13108.
7. Cooper, R.D.G. & Thompson, R.C. (1996) Semisynthetic glycopeptide antibiotics. *Annu. Report Med. Chem.* **31**, 131–140.
8. Juvvadi, P., Vunnam, S. & Merrifield, R.B. (1996) Synthetic melittin, its enantio, retro, and retroenantio isomers, and selected chimeric analogs: their antibacterial, hemolytic, and lipid bilayer action. *J. Am. Chem. Soc.* **118**, 8989–8997.
9. Blondelle, S. & Houghten, R.A. (1992) Progress in antimicrobial peptides. *Annu. Report Med. Chem.* **27**, 159–168.
10. Pinilla, C., Appel, J., Dooley, C., Blondelle, S., Eichler, J., Dörner, B., Ostresh, J. & Houghten, R.A. (1996) *Combinatorial Peptide and Nonpeptide Libraries* (Jung, G., ed.). VCH, New York.
11. Kondejewski, L.H., Farmer, S.W., Wishart, D.S., Kay, C.M., Hancock, R.E.W. & Hodges, R.S. (1996) Modulation of structure and antibacterial and hemolytic activity by ring size in cyclic gramicidin S analogs. *J. Biol. Chem.* **271**, 25261–25268.
12. Porter, E.A., Wang, X., Lee, H.-S., Weisblum, B. & Gellman, S.H. (2000) Antibiotics: non-haemolytic β-amino-acid oligomers. *Nature (Lond.)* **404**, 565.
13. Kondejewski, L.H., Farmer, S.W., Wishart, D.S., Hancock, R.E.W. & Hodges, R.S. (1996) Gramicidin S is active against both gram-positive and gram-negative bacteria. *Int. J. Peptides Protein Res.* **47**, 460–466.
14. Gause, G.F. & Brazhnikova, M.G. (1944) Gramicidin S and its use in the treatment of infected wounds. *Nature* **154**, 703.
15. Lambert, H.P. & O'Grady, F.W. (1992) *Antibiotics and Chemotherapy*, 6th edn, pp. 232–233. Churchill Livingstone, Edinburgh.
16. Ovchinnikov, Y.A. & Ivanov, V.T. (1975) Conformational states and biological activity of cyclic peptides. *Tetrahedron* **31**, 2177–2209.
17. Ando, S., Nishikawa, H., Takiguchi, H., Lee, S. & Sugihara, G. (1993) Antimicrobial specificity and hemolytic activity of cyclized basic amphiphilic β-structural model peptides and their interactions with phospholipid bilayers. *Biochem. Biophys. Acta* **1147**, 42–49.
18. Ando, S., Nishihama, M., Nishikawa, H., Takiguchi, H., Lee, S. & Sugihara, G. (1995) Drastic reduction of antimicrobial activity by replacement of Orn residues with Lys in cyclized amphiphilic β-structural model peptides. *Int. J. Peptide Protein Res.* **46**, 97–105.
19. Tamaki, M., Arai, I., Akabori, S. & Muramatsu, I. (1995) Role of ring size on the secondary structure and antibiotic activity of Gramicidin S. *Int. J. Peptide Protein Res.* **45**, 299–302.
20. Zidovetzki, R., Banerjee, U., Harrington, D.W. & Chan, S.I. (1988) NMR study of the interactions of polymyxin B, gramicidin S and valinomycin with dimyristoyllecithin bilayers. *Biochemistry* **27**, 5686–5692.
21. Prenner, E.J., Lewis, R.N.A.H., McElhaney, R.N., Kondejewski, L.H., Hodges, R.S., Neuman, K.C. & Gruner, S.M. (1997) Cubic phases induced upon interactions of gramicidin S with lipid bilayers. – a clue to its mechanism of action? *Biophys. J.* **72**, A191.
22. Waki, M. & Izumiya, N. (1990) Chemical synthesis and bioactivity of gramicidin S and related peptides. *Biochemistry of Peptide Antibiotics* (Kleinkauf, H. & von Döhren, H., eds). De Gruyter, Berlin.
23. Izumiya, N., Kato, T., Aoyagi, H., Waki, M. & Kondo, M. (1979) *Synthetic Aspects of Biologically Active Cyclic Peptides-Gramicidin S and Tyrocidines*. Halsted Press, New York.
24. Prenner, E.J., Lewis, R.N.A.H., Neuman, K.C., Gruner, S.M., Kondejewski, L.H., Hodges, R.S. & McElhaney, R.N. (1997) Nonlamellar phases induced by the interaction of Gramicidin S with lipid bilayers. A possible relationship to membrane-disrupting activity. *Biochemistry* **36**, 7906–7916.
25. Wu, M., Maier, E., Benz, R. & Hancock, R.E.W. (1999) Mechanism of interaction of different classes of cationic antimicrobial peptides with planar bilayers and with the cytoplasmic membrane of *Escherichia coli*. *Biochemistry* **38**, 7235–7242.
26. Nagai, U. & Sato, K. (1985) Synthesis of a bicyclic dipeptide with the shape of a β-turn central part. *Tetrahedron Lett.* **26**, 647–650.
27. Sato, K. & Nagai, U. (1986) Synthesis and antibiotic activity of a gramicidin S analogue containing bicyclic β-turn dipeptides. *J. Chem. Soc., Perkin Trans.* **I**, 1231–1234.
28. Bach, A.C., I.I.Markwalder, J.A. & Ripka, W.C. (1991) Synthesis and NMR conformation analysis of a β-turn mimic incorporated into gramicidin S. *Int. J. Peptide Protein Res.* **38**, 314–323.
29. Hanessian, S., McNaughton-Smith, G., Lombart, H.-G. & Lubell, W.D. (1997) Design and synthesis of conformationally constrained amino acids as versatile scaffolds and peptide mimetics. *Tetrahedron* **53**, 12789–12854.
30. Ripka, W.C., Delucca, G.V., Bach, A.C., Pottorf, R.S. & Blaney, J.M. (1993) Protein β-turn mimetics II: design, synthesis, and evaluation in the cyclic peptide gramicidin S. *Tetrahedron* **49**, 3609–3628.
31. Bach, A.C., I.I.Pottorf, R.S., Blaney, J.M., De Luca, G.V. & Ripka, W.C. (1994) Gramicidin S a general model for β-turn mimics? In: *Peptides Chemistry and Biology, Proceeding of the* 13th American Peptide Symposium. (Hodges, R.S. & Smith, J.A., eds) ESCOM Sci.,. Leiden, The Netherlands, pp. 284–286.
32. Graciani, N.R., Tsang, K.Y., McCutchen, S.L. & Kelly, J.W. (1994) Amino acids that specify structure through hydrophobic clustering and histidine–aromatic interactions lead to biologically active peptidomimetics. *Bioorg. Med. Chem.* **2**, 999–1006.
33. De la Figuera, N., Jiménez, M. A., Biacs, M., García-López, M. T., González-Muñiz, R., Andreu, D. (1995) Gramicidin S analogs containing the new β-turn dipeptide mimetic IBTM. In: *Peptides 1994 (Proceedings of the 23rd European Peptide Symposium)*, (Maia, H.L.S., ed.). ESCOM, Leiden, The Netherlands, pp. 702–703.
34. Andreu, D., Ruiz, S., Carreño, C., Alsina, J., Albericio, F., Jiménez, M.A., de la Figuera, N., Herranz, R., García-López, M.T. & González-Muñiz, R. (1997) IBTM-containing gramicidin S analogues: evidence for IBTM as a suitable type II′ β-turn mimetic. *J. Am. Chem. Soc.* **119**, 10579–10586.
35. Preliminary results: Lombart, H.-G. & Lubell, W.D. (1996) Use of Azabicycloalkane amino acids to stabilize β-turn conformations in model peptides and gramicidin S. In: *Peptides Chemistry, Structure and Biology* (Kaumaya, P.T.P. & Hodges, R.S., eds). ESCOM Sci., Leiden, The Netherlands, pp. 695–696.
36. Lombart, H.-G. & Lubell, W.D. (1994) Synthesis of enantiopure α,ω-diamino dicarboxylates and azabicycloalkane amino acids by Claisen condensation of α-*N*-(phenylfluorenyl) amino dicarboxylates. *J. Org. Chem.* **59**, 6147–6149.
37. Lombart, H.-G. & Lubell, W.D. (1996) Rigid dipeptide mimetics: efficient synthesis of enantiopure indolizidinone amino acids. *J. Org. Chem.* **61**, 9437–9446.
38. Waldmann, H. & Kunz, H. (1983) Allyester als selektiv abspaltbare Carboxyschutzgruppen in der Peptid- und *N*-Glycopeptidsynthese. *Liebigs Ann. Chem.* 1712–1725.
39. Dourtoglou, V., Gross, B., Lambropoulou, V. & Zioudrou, C. (1984) *O*-Benzotriazolyl-*N*,*N*,*N*′,*N*′-tetramethyuronium hexafluorophosphate as coupling reagent for the synthesis of peptides of biological interest. *Synthesis* 572–574.

40. Knorr, R., Trzeciak, A., Bannwarth, W. & Gillessen, D. (1989) New coupling reagents in peptide chemistry. *Tetrahedron Lett.* **30**, 1927–1930.
41. Abdelmoty, I., Albericio, F., Carpino, L.A., Foxman, B. & Kates, S.A. (1994) Structural studies of reagents for peptide bond formation: Crystal and molecular structures of HBTU and HATU. *Lett. Peptide Sci.* **1**, 57–67.
42. Friedrich-Bochnitschek, S., Waldmann, H. & Kunz, H. (1989) Allyl esters as carboxy protecting groups in the synthesis of *O*-glycopeptides. *J. Org. Chem.* **54**, 751–756.
43. Ösapay, G., Profit, A. & Taylor, J.W. (1990) Synthesis of tyrocidine A: use of oxime resin for peptide chain assembly and cyclization. *Tetrahedron Lett.* **31**, 6121–6124.
44. Mihara, H., Hayashida, J., Hasegawa, H., Ogawa, H.I., Fujimoto, T. & Nishino, N. (1997) A pair of pyrene groups as a conformational probe for antiparallel β-sheet structure formed in cyclic peptides. *J. Chem. Soc., Perkin Trans.* **II**, 517–522.
45. Arai, T., Imachi, T., Kato, T., Ogawa, H.I., Fujimoto, T. & Nishino, N. (1996) Synthesis of [hexafluorovalyl$^{1,1'}$]gramicidin S. *Bull. Chem. Soc. Jpn.* **69**, 1383–1389.
46. Van Maarseveen, J.H. (1998) Solid phase synthesis of heterocycles by cyclization/cleavage methodologies. *Comb. Chem. High Throughput Screening* **1**, 185–214.
47. Kaiser, E.T., Mihara, H., Laforet, G.A., Kelley, J.W., Walters, L., Findeis, M.A. & Sasaki, T. (1989) Peptide and protein synthesis by segment synthesis-condensation. *Science* **243**, 187–191.
48. Kawai, K. & Nagai, U. (1978) Comparison of conformation and antimicrobial activity of synthetic analogs of gramicidin S: stereochemical consideration of the role of D-phenylalanine in the antibiotic. *Biopolymers* **17**, 1549–1565.
49. Woody, R.W. (1995) Circular dichroism. *Methods Enzymol.* **246**, 34–71.
50. Wütrich, K. (1986) In: *NMR of Proteins and Nucleic Acids*. Wiley, New York, pp. 117–175.
51. Kessler, H. (1982) Conformation and biological activity of cyclic peptides. *Angew. Chem. Int. Ed. Engl.* **21**, 512–523.
52. Bystrov, V.F., Ivanov, V.T., Portnova, S.L., Balashova, T.A. & Ovchinnikov, Y.A. (1973) Refinement of the angular dependence of the peptide vicinal NH-C$^{\alpha}$H coupling constant. *Tetrahedron* **29**, 873–877.
53. Tamaki, M., Araki, M., Okitsu, T., Sakamoto, H., Takimoto, M. & Muramatsu, I. (1985) Synthesis and properties of gramicidin S analogs containing D-Phe-L-Pro-D-Val or L-Phe-L-Pro-D-Val sequences in place of D-Phe-L-Pro-L-Val sequence in the β-turn part of the antibiotic. *Bull. Chem. Soc. Jpn.* **58**, 531–535.
54. Sato, K., Kato, R. & Nagai, U. (1986) Studies on β-Turn of peptides. XII. Synthetic confirmation of weak activity of [D-Pro$^{5,5'}$]-gramicidin S predicted from β-turn preference of its partial sequence. *Bull. Chem. Soc. Jpn.* **59**, 535–538.
55. Nagai, U. & Sato, K. (1983) Studies on the β-turn of peptides. VII. Synthesis and antibiotic activities of gramicidin S analogs with L-Pro-L-Asn or L-Pro-D-Ala sequence at the β-turn part. *Bull. Chem. Soc. Jpn.* **56**, 3329–3336.
56. Tamaki, M., Araki, M., Okitsu, T., Sakamoto, H., Takimoto, M. & Muramatsu, I. (1985) Synthesis and properties of gramicidin S analogs containing Pro-D-Phe sequence in place of D-Phe-Pro sequence in the β-turn part of the antibiotic. *Bull. Chem. Soc. Jpn.* **58**, 1469–1472.
57. Haque, T.S., Little, J.C. & Gellman, S.H. (1994) 'Mirror image' reverse turns promote β-hairpin formation. *J. Am. Chem. Soc.* **116**, 4105–4106 and refs therein.
58. Sibanda, B.L. & Thornton, J.M. (1985) β-Hairpin families in globular proteins. *Nature* **316**, 170–174.
59. Takeuchi, Y. & Marshall, G.R. (1998) Conformational analysis of reverse-turn constraints by *N*-methylation and *N*-hydroxylation of amide bonds in peptides and non-peptide mimetics. *J. Am. Chem. Soc.* **120**, 5363–5372.
60. Estiarte, M.A., Rubiralta, M., Diez, A., Thormann, M. & Giralt, E. (2000) Oxazolopiperid-2-ones as type II' β-turn mimetics: synthesis and conformational analysis. *J. Org. Chem.* **65**, 6992–6999.
61. Kaiser, E., Colescott, R.L., Bossinger, C.D. & Cook, P.L. (1970) Color test for detection of free terminal amino groups in the solid-phase synthesis of peptides. *Anal. Biochem.* **34**, 595–598.